Available online at www.sciencedirect.com
SCIENCE DIRECT®
Biochemical and Biophysical Research Communications 327 (2005) 174–182
BBRC
www.elsevier.com/locate/ybbrc

Interaction analysis of chimeric metal-binding green fluorescent protein and artificial solid-supported lipid membrane by quartz crystal microbalance and atomic force microscopy

Virapong Prachayasittikul[a,*], Chartchalerm Isarankura Na Ayudhya[a,b], Lutz Hilterhaus[b], Andreas Hinz[b], Tanawut Tantimongcolwat[a,b], Hans-Joachim Galla[b,*]

[a] *Department of Clinical Microbiology, Faculty of Medical Technology, Mahidol University, Bangkok 10700, Thailand*
[b] *Institute of Biochemistry, Westfälische Wilhelms Universität, 48149 Muenster, Germany*

Received 23 November 2004
Available online 9 December 2004

Abstract

Non-specific adsorption and specific interaction between a chimeric green fluorescent protein (GFP) carrying metal-binding region and the immobilized zinc ions on artificial solid-supported lipid membranes was investigated using the quartz crystal microbalance technique and the atomic force microscopy (AFM). Supported lipid bilayer, composed of octanethiol and 1,2-dipalmitoyl-*sn*-glycero-3-phosphocholine/1,2-dioleoyl-*sn*-glycero-3-[*N*-(5-amino-1-carboxypentyl iminodiacetic acid)succinyl] (NTA-DOGS)-Zn^{2+}, was formed on the gold electrode of quartz resonator (5 MHz). Binding of the chimeric GFP to zinc ions resulted in a rapid decrease of resonance frequency. Reversibility of the process was demonstrated via the removal of metal ions by EDTA. Nanoscale structural orientation of the chimeric GFP on the membrane was imaged by AFM. Association constant of the specific binding to metal ions was 2- to 3-fold higher than that of the non-specific adsorption, which was caused by the fluidization effect of the metal-chelating lipid molecules as well as the steric hindrance effect. This infers a possibility for a further development of biofunctionalized membrane. However, maximization is needed in order to attain closer advancement to a membrane-based sensor device.

Keywords: Quartz crystal microbalance; Green fluorescent protein; Atomic force microscopy; Hexahistidine; Metal-chelating lipid; Functionalized membrane; Protein–lipid interaction

Functionalized membranes are extensively applied as biological devices, templates for structural determination, and model to study molecular recognition and transport processes. Lipid is suitable as coating material owing to its homogeneity and stability. Self-organization into monolayer or bilayer of the lipid reveals a feasibility of developing membrane-based sensor device. Furthermore, it can be transferred onto various kinds of solid support by Langmuir–Blodgett technique or vesicle fusion. Lipid interfaces can be functionalized by reconstitution of membrane proteins or incorporation of reactive compounds via covalent coupling or specific ligand–receptor binding [1–3].

In recent decade, binding interaction between ligands and receptors on an artificial membrane has come into an attention in various aspects aiming to gain further application on biological recognition and molecular engineering. For instance, the specific binding of avidin to biotin containing lipid lamella surfaces has thoroughly been investigated [4]. Binding of annexin to lipid membranes containing anionic phospholipids in a calcium-dependent manner has extensively been reported [5–7]. The high affinity binding of histidine

* Corresponding authors. Fax: +662 849 6330 (V. Prachayasittikul), +49 251 8333206 (H.-J. Galla).
E-mail addresses: mtvpr@mahidol.ac.th (V. Prachayasittikul), gallah@uni-muenster.de (H.-J. Galla).

0006-291X/$ - see front matter © 2004 Elsevier Inc. All rights reserved.
doi:10.1016/j.bbrc.2004.11.150

residues to immobilized divalent cations on chelating lipid membrane opens up a potential approach for reversible immobilization of proteins [1,8,9]. Two-dimensional crystallization of many kinds of proteins has been obtained by specific binding on the lipid layer [10,11].

Green fluorescent protein (GFP) is an autofluorescent protein isolated from the jellyfish, *Aequorea victoria*. The GFP has been progressively applied for both in vivo and in vitro studies of cellular processes, e.g., as reporters of localization, gene expression, protein trafficking, and protein–protein interaction [12–17]. Recently, a combination of GFP with highly sensitive techniques has revolutionized the membrane-based sensor [18–20]. However, it remains necessary to perceive more of the binding interaction between the GFP and other biomolecules especially various kinds of lipids. Association and organization of the chimeric GFPs to lipid membrane has individually been investigated via various biophysical techniques [8,9,21]. However, more detail of their quantitative interaction is needed to be explored for further application.

Quartz crystal microbalance (QCM) is known as a simple and low-cost mass sensing technique basing on the piezoelectric effect. The QCM has extensively been applied as a powerful device to study adsorption processes at solid–liquid interfaces in both chemical and biological research [22–25]. This technique provides a wide range of detection. It can detect not only surface coverage by small molecules or polymer films but it is also capable of determining much larger masses bound to the surface including complex arrays of biopolymers, biomacromolecules or whole cells. As compared to other systems, the QCM offers a rapid response while obviating the need for additive labeling reagents and permits direct conversion of a frequency signal into mass accumulation. Among other measurements, atomic force microscopy (AFM) is a powerful technique for high resolution surface studies of biological macromolecules (e.g., DNA and proteins). It can be operated under aqueous condition so that real time monitoring can be performed [26]. However, Langmuir film balance is a biophysical technique used for analysis and manipulation of monomolecular organic layers such as amphiphilic molecules, fatty acids, and lipids [27].

Therefore, in this study, we use the QCM to study the molecular interaction of the chimeric GFP with artificial solid-supported bilayer membrane. This biomimetic material has been applied as a model to study adsorption behavior of the GFP to lipid membrane. Adsorption of the protein on the lipid monolayer has also been determined by film balance measurement for comparison. In parallel, specific recognition of the chimeric GFP carrying hexapolyhistidine to metal portion immobilized onto the membrane has been identified. Specific orientation on the desired membrane has been visualized via AFM in corresponding to the adsorption characteristic. Furthermore, association constant between the chimeric His6GFP and immobilized metal ions has been calculated in order to explore the feasibility of applying the biofunctionalized membrane-based analytical devices for future metal determination.

Materials and methods

Lipid and chemicals. 1,2-Dipalmitoyl-*sn*-glycero-3-phosphocholine (DPPC) and 1,2-dioleoyl-*sn*-glycero-3-[*N*-(5-amino-1-carboxypentyl iminodiacetic acid)succinyl] (NTA-DOGS) were purchased from Avanti Polar Lipids (Alabaster, AL, USA). Octanethiol was from Fluka (Neu Ulm, FRG). Water was first purified through a Millipore water purification Milli-Q RO 10 Plus (Millipore GmbH, Eschborn, FRG) and then finally with the Millipore ultrapure system Milli-Q Plus 185 (18.2 $M\Omega\,cm^{-1}$). The 5 MHz overtone polished AT-cut quartz crystals (plano–plano) were obtained from KVG (Niederbischofsheim, FRG), the silver conductive adhesive was from Epoxy-GmbH (Fürth/Odenwald, FRG), and the silicon glue (Elchsiegel) was from Rhône Poulenc (Leverkusen, FRG). Gold (99.99% purity) applied for the gold electrodes was a generous gift from DEGUSSA (Hanau, FRG), while the chromium was purchased from Bal-Tec (Balzers, Liechtenstein). For all experiments, phosphate-buffered saline (50 mM Na_2HPO_4, 0.3 M NaCl, pH 7.4; PBS) was used. Lipid stock solution was prepared by dissolving powdered lipid in chloroform.

Proteins. Chimeric green fluorescent protein carrying hexapolyhistidine (His6GFP) was expressed in *Escherichia coli* strain TG1 and further purified to homogeneity via immobilized metal affinity chromatography (IMAC) charged with zinc ions as previously described [28,29]. Protein concentration was determined by UV absorption with $\varepsilon_{395\ nm} = 27{,}000\ M^{-1}\,cm^{-1}$ and protein purity was analyzed by SDS–PAGE.

Vesicle preparation. Lipid film of mixed DPPC with various amounts of the NTA-DOGS was prepared by drying the lipids dissolved in chloroform under nitrogen stream followed by 2 h incubation under vacuum at 50 °C. The lipid film was stored at 4 °C until use. Multilamellar vesicles (MLVs) were prepared by first swelling the lipid film in PBS followed by periodically vortexing for 30 s for 4–5 times. The resulting MLVs were subsequently converted into large unilamellar vesicles (LUVs) by pressing the MLVs through a polycarbonate membrane (100 nm pore diameter) via a miniextruder (LiposoFast: Avestin, Ottawa, Canada).

Impedance analysis. The electrochemical cell consisted of a quartz crystal with one gold electrode serving as working electrode and a platinum wire as counter electrode. AC impedance spectroscopy was carried out with an impedance gain/phase analyzer SI 1260 from Solartron instruments (Farnborough, Great Britain). The magnitude of the impedance $|Z(f)|$ as well as the phase angle $F(f)$ was recorded in the frequency range of 10^{-1}–10^{6} Hz with an AC amplitude of 30 and 0 mV DC offset potential. Quantitative analysis of the spectra was performed by fitting all the parameters of the equivalent circuit to the data by a nonlinear-least squares fit using the Levenberg–Marquardt algorithm. The equivalent circuit used for the fitting procedure simply consisted of a resistance in series with a capacitance. The resistance represented the ohmic nature of the electrolyte and the capacitance represented the electrical behavior of the membrane. The resistances of monolayer and bilayer were not detectable in the applied frequency range and were therefore neglected in the analysis.

Preparation of solid-supported bilayer on gold electrode. Gold electrodes with an area of 0.265 cm^2 were deposited on each side of a quartz plate by means of an evaporation unit (E 306, Edwards, UK), by using a suitable mask design. After application of a layer of chromium (10 ± 20 nm) to improve the adhesion of gold, the gold layer was subsequently deposited with a final thickness of about 200 nm. Prior to

use, they were cleaned in both of the piranha solution (60 ml conc. H_2SO_4, 20 ml of 30% H_2O_2) and high-energy argon plasma (plasma cleaner, Harrick, USA) for 5–10 min before placing the quartz plate in the teflon chamber. The quartz surface was then immersed for 30 min in an ethanolic solution containing 1 mM octanethiol. Subsequently, the electrode was extensively rinsed several times with ethanol to remove remaining thiols and then at least five times with buffer to remove ethanol. Formation of the first monolayer was verified via impedance analysis. The bilayer was formed by adding the preformed vesicles of either pure DPPC or mixture of DPPC:NTA-DOGS to the hydrophobic monolayer of octanethiol in PBS for 1 h at 50 °C to induce fusion process. The electrodes were subsequently stored at room temperature for overnight to achieve a complete fusion. Remaining vesicles were removed by rinsing the electrode surface several times with buffer solution. Finally, the impedance spectroscopy was again applied to ensure proper formation of an insulating phospholipid monolayer.

Quartz crystal microbalance measurement. Experimental setup for the QCM measurement used in this study is depicted schematically in Fig. 1A. Basically, it consisted of the quartz resonator, a flow system, and the oscillator circuit. The gold electrodes were connected to the oscillator circuit via thin silver wires, which were fixed on the gold electrodes by a conductive adhesive. The quartz plates were mounted into a teflon holder designed to allow the aqueous solution to contact only with the gold-coated surface of the quartz crystal. An inlet and outlet allowed for a continuous buffer flow as well as protein addition by using a peristaltic pump. The whole flow system included a volume of 2 ml pumped with a flow rate of 1.36 ml min^{-1} through the quartz chamber. The crystal and the oscillator circuit were placed in a temperature-controlled chamber, which served as a water-jacketed Faraday cage for maintaining the temperature constant at 20 °C. The oscillator circuit consisted of an integrated circuit SN74LS124N from Texas Instruments connected to a frequency counter from Hewlett Packard (HP 53181 A). The frequency signal was transferred to the personal computer via the data acquisition board (DAQ; National Instruments, München, FRG).

Film balance measurement. Film balance measurement was performed as previously described [8]. Briefly, phospholipid films of DPPC or DPPC:NTA-DOGS at various ratios were prepared from a lipid stock solution by carefully spreading via a microsyringe at the air/liquid interface. After an equilibration time of 10 min, the film was compressed until the final surface pressure reached 25 mN m^{-1}. The interface was allowed to equilibrate for at least 45 min, at which point no further barrier movement was required to maintain constant pressure. The chimeric His6GFP dissolved in PBS was then injected into the subphase underneath the monolayer to yield subphase concentration of 72 nM. Changes of the lateral pressure after injection were measured at constant interfacial area and recorded for a minimum of 60 min.

Preparation of Langmuir–Blodgett bilayer on mica. Langmuir–Blodgett (LB) films were prepared as previously described [9]. DPPC was spread on the buffer subphase and the lipid film was compressed to a surface pressure of 45 mN m^{-1} at the subphase temperature of 20 °C. The DPPC monolayer was transferred to a freshly cleaved mica sheet. The monolayer film was allowed to dry in air for overnight. Second monolayer composed of DPPC, DPPC/NTA-DOGS or DPPC/NTA-DOGS-Zn^{2+} at various ratios was compressed to 30 mN m^{-1} and then the His6GFP was injected underneath the lipid monolayer to yield the

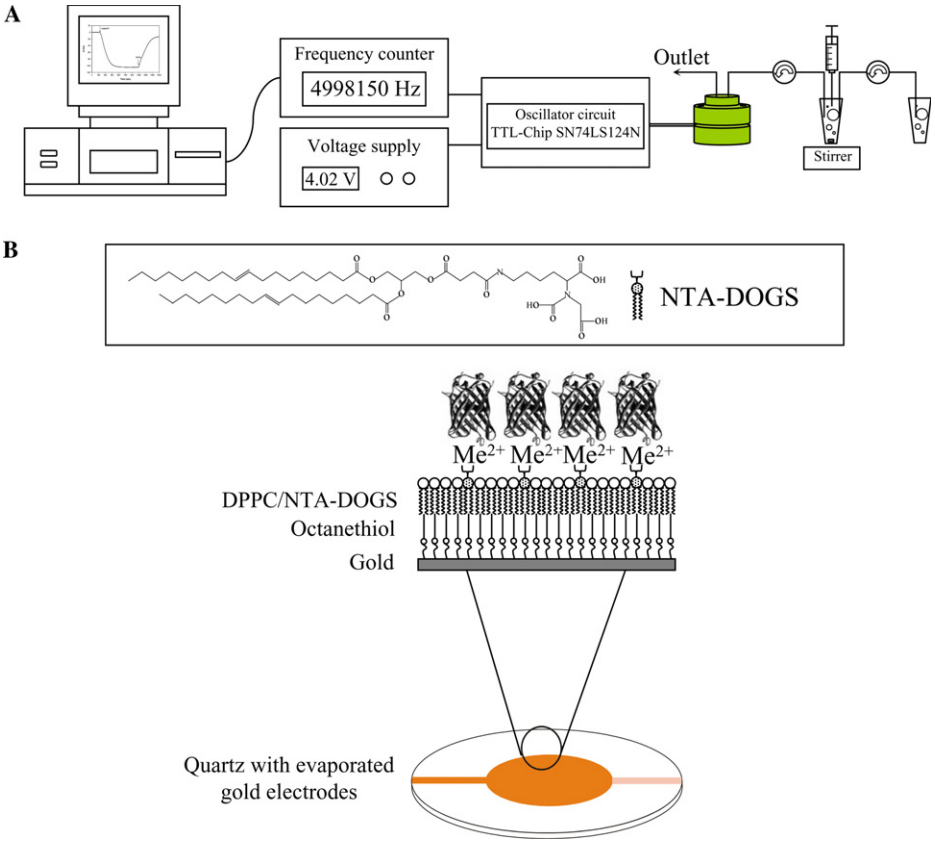

Fig. 1. (A) Experimental setup of the quartz crystal microbalance based on the flow injection system. (B) Schematic representation of a specific binding of chimeric His6GFP onto a functionalized quartz surface with an immobilized lipid bilayer composed of an octanethiol monolayer and a physisorbed metal-chelating lipid monolayer (DPPC:NTA-DOGS).

subphase concentration of 72 nM. The lipid–protein mixture was subsequently deposited onto the first hydrophobic DPPC monolayer at the desired pressure, and the mica sheet was transferred into an open fluid cell under buffer solution.

Atomic force microscopy measurement. Topographical images of solid-supported membranes were obtained via an atomic force microscope (Nanoscope IIIa Bioscope: Digital Instruments, Santa Barbara, USA) operating in contact mode as described in detail elsewhere [9]. Multiple cross-sections of the individual protein images by AFM were performed and the mean height of protein domain was analyzed by the WSxM software (Nanotec Electronica, Madrid, Spain).

Results and discussion

The GFP has extensively been applied in an attempt to develop artificial membrane-based fluorescent sensor in several studies [8,18]. Even though nanoscale orientation has been explored by our group upon the interaction between chimeric metal-binding GFP and lipid membrane [9]. However, we herein report for the first time on the interaction of the chimeric GFP onto artificial solid-supported lipid membrane using a combination of QCM, Langmuir film balance, and AFM.

Formation of solid-supported membrane on quartz crystal

Solid-supported lipid bilayer has extensively been utilized in fundamental biophysical research and biosensor applications [30–33]. In this study, the solid-supported membrane was created and further investigated for lipid–protein interaction via the quartz resonator. The monolayer of octanethiols (OT) was coated onto the gold electrode via self-assembled monolayers (SAMs) technique. The closely packed hydrocarbon chains of OT promoted attachment of a second lipid layer onto the hydrophobic surface achieving a bilayer membrane. Therefore, mixtures of DPPC and metal-chelating lipid (NTA-DOGS) at various ratios were successfully physisorbed on top of the OT-layer by vesicle fusion (Fig. 1B). Characteristic of electrical parameters of the OT monolayer as well as the lipid bilayer was verified by means of impedance spectroscopy. Fig. 2 demonstrates typical impedance spectra of the monolayer and bilayer formation. The equivalent circuit composed of a capacitance (C_m; represented the OT monolayer and the phospholipid bilayer), in series to an Ohmic resistance (R_e; represented the bulk resistance and the wire connections). This equivalent circuit is valid, since the OT forms almost defect-free monolayer, leading to a sole capacitive behavior in the observed frequency range [32]. The solid lines denote the fitting results according to the equivalent circuit. Mean capacitance of the OT-monolayer and the OT/DPPC:NTA-DOGS was 2.5 and 1.2 μF cm^{-2}, respectively. This ensures that the metal-chelating lipid membrane has been successfully deposited on the surface of quartz resonator with 95% surface coverage [32].

Fluidization effect of metal-chelating lipid on adsorption of the chimeric His6GFP to lipid monolayer and bilayer

The QCM was applied to monitor both the adsorption of the His6GFP onto lipid membrane and the specific binding to metal ions with high resolution basing on the piezoelectric effect. Fig. 3 illustrates the time

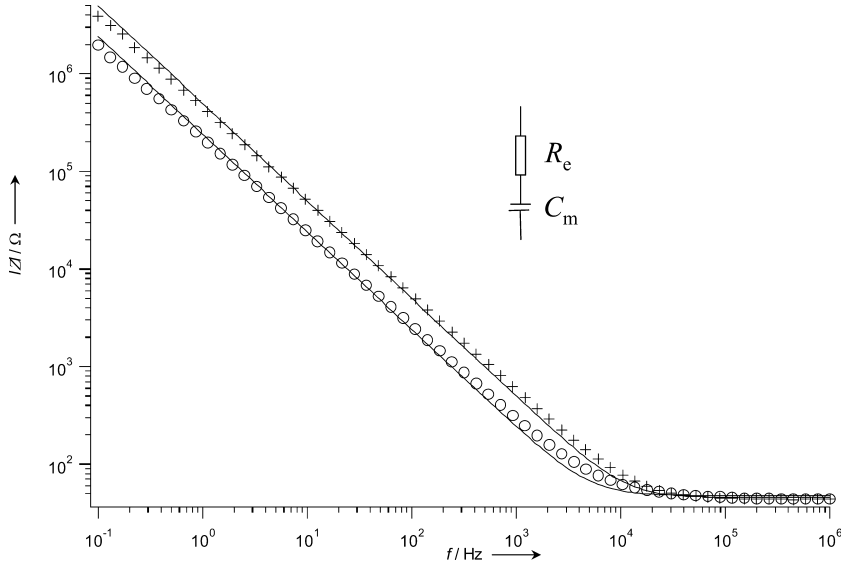

Fig. 2. Impedance spectra of a chemisorbed monolayer of octanethiol (OT) and a bilayer consisting of OT and a second physisorbed monolayer of DPPC or DPPC:NTA-DOGS. The solid lines are the results of the fitting procedure according to the Levenberg–Marquardt algorithm with the following parameters: $C_{OT} = 2.5$ μF cm^{-2}, $C_{OT/DPPC:NTA\text{-}DOGS} = 1.2$ μF cm^{-2}. The equivalent circuit in the inset was used for impedance data evaluation. C_m represents the capacitance of the octanethiol monolayer and the bilayer composed of the octanethiol and a phospholipid, respectively, and R_e represents the Ohmic resistance of the electrolyte and the wire connections.

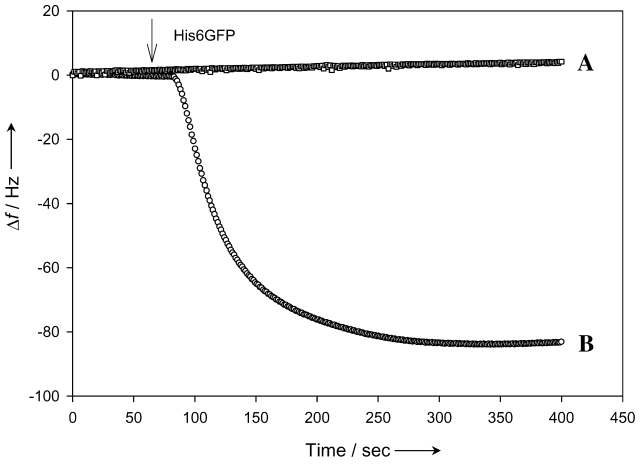

Fig. 3. Time course of the resonance frequency shift upon adsorption of the chimeric His6GFP onto a bilayer of OT and DPPC:NTA-DOGS (line B) or DPPC (line A).

course of the shift of resonance frequency upon adsorption of the His6GFP to the lipid mixture (DPPC:NTA-DOGS; 4:1). At a constant resonance frequency, protein solution was injected into a small vessel and the frequency change was monitored. Adsorption of the His6GFP (0.165 nM) to the metal-chelating lipid membrane revealed a rapid decrease of the frequency up to 82 Hz while no frequency change was observed on the DPPC membrane. This shows the low adsorptivity of the protein to the rigid domain of DPPC. Contrarily, the fluidization effect caused by the metal-chelating lipid facilitates non-specific protein adsorption.

Question was arisen whether the NTA-DOGS content, which influenced fluidity of the membrane, would affect the adsorption of His6GFP. Various ratios of lipid mixture of the lipid bilayer were formed on the quartz plates. Fig. 4A shows the relation between the frequency changes and the metal-chelating lipid contents. Increase of frequency change corresponding to the amount of NTA-DOGS peaked at the ratio of 6:1, generating the highest frequency change of 105 Hz. Further addition of NTA-DOGS resulted in a gradual decrease of response.

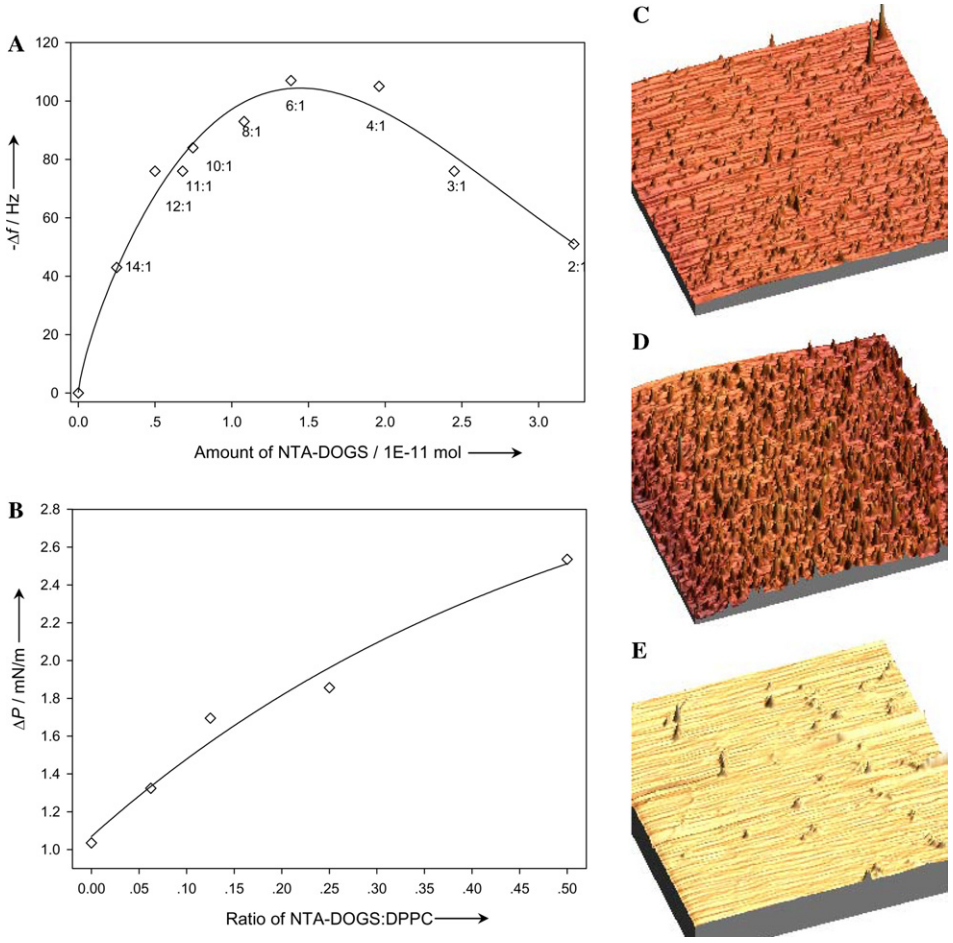

Fig. 4. (A) Resonance frequency change (Δ*f*) upon adsorption of chimeric His6GFP onto lipid bilayer membrane composed of various ratios of DPPC and NTA-DOGS immobilized on quartz surface. (B) Increasing of delta pressure upon adsorption of chimeric His6GFP on various ratios of DPPC:NTA-DOGS monolayers determined by film balance measurement. (C–E) Topographical images of non-specific adsorption of chimeric His6GFP onto DPPC:NTA-DOGS membranes at ratios of 2:1 (C), 6:1 (D), and pure DPPC (E).

To test whether such adsorption phenomenon would be generated on the lipid monolayer, film balance technique was then applied for investigation. The lipid mixture was prepared and lateral pressure was kept constant at 25 mN m^{-1}. The His6GFP (72 nM) was then injected beneath the monolayer membrane. At the desired pressure, degree of adsorption was monitored by increasing interfacial pressure with time. Change in magnitude of the interfacial pressure was corresponding to the amount of NTA-DOGS (Fig. 4B). Increasing of NTA-DOGS resulted in high fluidization of the lipid membrane, which in turn enhanced the multilayer protein adsorption. This adsorption provoked an enlargement of interfacial pressure (Fig. 4B) while the protein lost the fluorescence property upon exposure to the high surface pressure at the air/water interface [1,8].

The correspondence between adsorption of the His6GFP and amount of NTA-DOGS was directly confirmed as shown by the AFM (Figs. 4C–E). Individual lipid mixture at ratios of 6:1, 2:1, and pure DPPC was spread onto the buffer subphase and the interfacial pressure was compressed until 30 mN m^{-1}. The His6GFP was injected into the subphase underneath the lipid monolayer to yield a final concentration of 72 nM. The lipid–protein mixture was subsequently transferred to the DPPC-coated mica sheet and investigated under the AFM. Fig. 4C shows the topographic images of non-specific adsorption of the His6GFP onto the lipid mixture at a ratio of 2:1. The non-homogeneous distribution of the knobs appeared on the flat surface was revealed. The height of these knobs composed of two groups with equal distribution was 1–3.5 and 6–18 nm. It is noteworthy that this small surface coverage was attributable to the steric hindrance effect of protein–protein interaction [4,34]. Meanwhile, marked increase of knob with the height approximately 2.5–5 nm (>95%) was perceived in the case of lipid mixture of 6:1 (Fig. 4D). Small amount of protein adsorption with the height of 2–3 nm was observed on the pure DPPC membrane (Fig. 4E). Such findings were correspondingly in agreement with the drop of frequency of QCM measurement (Fig. 4A).

Specific binding of the chimeric His6GFP onto immobilized metal ions on lipid bilayer membrane

To test whether by standing of metal ions on the NTA-DOGS membrane provided a specific binding to the His6GFP, zinc ions were loaded onto the immobilized lipid membrane on the QCM. Excess amount of zinc ions was removed by washing with phosphate buffer. Fig. 5 represents the time course of resonance frequency shift upon binding of the His6GFP. A rapid decrease of frequency was detected after injection of the His6GFP with a typical exponential decay. In addition, the metal-binding complex provided a stable signal

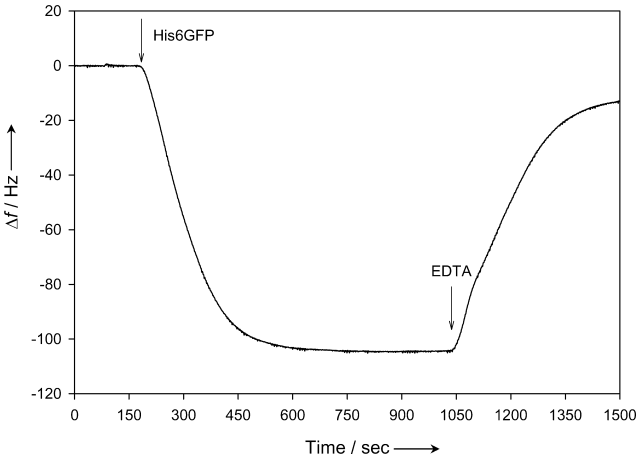

Fig. 5. Time course of the resonance frequency shift after binding of the chimeric His6GFP onto a bilayer of OT and DPPC:NTA-DOGS (4:1) charged with zinc ions. The first and second arrows indicate the time of protein addition and injection of EDTA solution, respectively.

change as compared to the non-specific adsorption (data not shown). After equilibrium was reached, EDTA containing buffer was then added to displace the zinc ions. This chelation effect regained the frequency up to 90 Hz indicating that 85% decrease of the initial frequency was caused by the specific binding of the protein.

To further obtain the association constant between protein and lipid membrane, the changes of resonance frequency were detected under various concentrations of His6GFP. Fig. 6 shows a binding isotherm of the His6GFP to immobilized zinc ions on the lipid membrane compared with non-specific adsorption. The solid lines are the results of the fitting procedures. In the presence of 0.05 nmol of His6GFP, the frequency changes

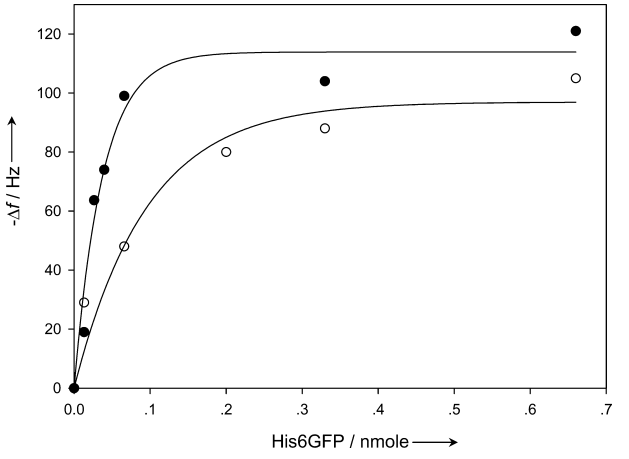

Fig. 6. Binding isotherm of the chimeric His6GFP on the metal-chelating lipid (NTA-DOGS) immobilized onto the quartz crystal resonator in the absence (open circle) or presence (filled circle) of zinc ions. The solid lines represent the fitting results according to the Langmuir adsorption isotherm with the following parameters: (○) $K_a = (13.5 \pm 4.11 \times 10^9)\ M^{-1}$, $\Delta f_{max} = -(111.62 \pm 8.67)$ Hz, (●) $K_a = (33.7 \pm 9.9 \times 10^9)\ M^{-1}$, $\Delta f_{max} = -(124.3 \pm 10.1)$ Hz.

were at 80 and 42 Hz for the specific binding to zinc and non-specific adsorption, respectively. Gradual increase of frequency change corresponding to the increase of chimeric protein until saturation was observed. The association constant was calculated by fitting the data to the Langmuir adsorption isotherm. The association constant of the immobilized zinc ions and the His6GFP was $33.7 \pm 9.9 \times 10^{-9}$ M, which was 2- to 3-fold higher than that of the non-specific adsorption ($K_a = 13.5 \pm 4.11 \times 10^{-9}$ M). Such evidences indicate stronger binding of specific polyhistidine to the chelated lipid membrane, which can be reversed by the chelating effect of EDTA. This specific association infers a potential of the chimeric GFP for a biofunctionalized membrane and development of sensor.

Molecular orientation of the chimeric GFP on the membrane was further observed via the AFM (Fig. 7). In the absence of zinc, the His6GFP tended to aggregate to form multilayer adsorption as evidenced by the non-spherical knob shape and heterogeneous scattering of the protein on the membrane (Fig. 7A). By contrast, the His6GFP preferentially bound to the immobilized zinc in a specific manner rather than aggregation. This was evidenced by distribution of the round-shaped knobs on the membrane (Fig. 7B). Furthermore, the height of the knob was approximately 4–5 nm, which corresponded to the height of the end on the side of green fluorescent protein (~4.2 nm). More importantly, interaction between hexahistidine and metal portion promotes a specific orientation and lateral organization in which strong fluorescence emission has been observed even under high interfacial pressure. This fluorescence rapidly disappears upon chelation of the metal by EDTA [8].

Further perspectives are needed to be taken into account for the significance of specific binding of only 2- to 3-fold higher of the His6GFP and the immobilized zinc as compared to the non-specific adsorption. First, small surface area of quartz crystal limits the amount of zinc ions on the NTA-DOGS ($\sim 1.96 \times 10^{-11}$ mol), which directly affects the low amount of the His6GFP to the ligand. Second, the protein-binding cavity calculated per lipid molecule restrains the specific binding to metal ions owing to the steric hindrance effect. Third, the non-specific binding can easily be potentiated by the charged macromolecular amphiphilic nature of the protein, which provides a tendency to migrate and to adsorb onto the QCM surface [35]. Fourth, fluidity of chelating lipid promotes a remarkable protein adsorption, which in turn raises the background binding constant up to nanomolar level. This level is 1000-fold higher than that of the binding constant between His6GFP and nickel ions determined by surface plasmon resonance [1]. However, the two latter effects may possibly circumvent by the future development of the metal-chelating lipid in the part of solid or rigid domain.

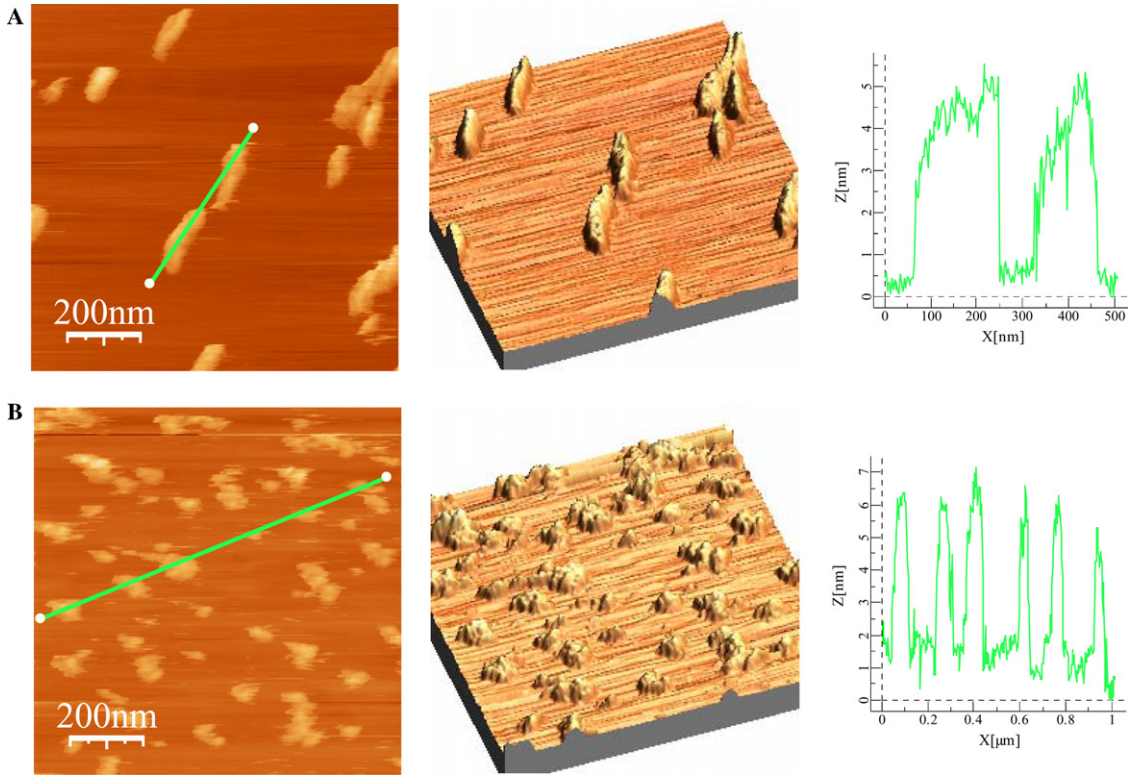

Fig. 7. Topographical images of a DPPC-DPPC:NTA-DOGS (4:1) Langmuir–Blodgett bilayer obtained in contact mode AFM and height analysis after addition of 72 nM His6GFP onto the lipid bilayer in the absence (A) and presence (B) of zinc ions. The image size was 1×1 μm^2.

Therefore, further optimization of the system needs to be performed in order to achieve not only the high binding constant but also explore more feasibility to further develop a membrane-based sensor device, particularly on metal determination [36–38].

Acknowledgments

This work was supported by the Deutsche Forschungsgemeinschaft (DFG) and the Bundesministerium für wirtschaftliche Zusammenarbeit und Entwicklung (Federal Ministry for Economic Co-operation and Development; BMZ) (Grant No. GA233/19-1,2). This project was also partially supported by the Thailand Toray Science Foundation (TTSF) and a grant from the annual budget of Mahidol University (B.E.2547).

References

[1] I.T. Dorn, K. Pawlitschko, S.C. Pettinger, R. Tampe, Orientation and two-dimensional organization of proteins at chelator lipid interfaces, Biol. Chem. 379 (1998) 1151–1159.
[2] D.Y. Sasaki, T.A. Waggoner, J.A. Last, T.M. Alam, Crown ether functionalized lipid membranes: lead ion recognition and molecular reorganization, Langmuir 18 (2002) 3714–3721.
[3] J.A. Last, T.A. Waggoner, D.Y. Sasaki, Lipid membrane reorganization induced by chemical recognition, Biophys. J. 81 (2001) 2737–2742.
[4] Z. Liu, H. Qin, C. Xiao, C. Wen, S. Wang, S.F. Sui, Specific binding of avidin to biotin containing lipid lamella surfaces studied with monolayers and liposomes, Eur. Biophys. J. 24 (1995) 31–38.
[5] A. Janshoff, M. Ross, V. Gerke, C. Steinem, Visualization of annexin I binding to calcium-induced phosphatidylserine domains, Chembiochem 2 (2001) 587–590.
[6] K. Kastl, M. Ross, V. Gerke, C. Steinem, Kinetics and thermodynamics of annexin A1 binding to solid-supported membranes: a QCM study, Biochemistry 41 (2002) 10087–10094.
[7] M. Ross, V. Gerke, C. Steinem, Membrane composition affects the reversibility of annexin A2t binding to solid supported membranes: a QCM study, Biochemistry 42 (2003) 3131–3141.
[8] C. Isarankura Na Ayudhya, V. Prachayasittikul, H.J. Galla, Binding of chimeric metal-binding green fluorescent protein to lipid monolayer, Eur. Biophys. J. 33 (2004) 522–534.
[9] V. Prachayasittikul, C. Isarankura Na Ayudhya, T. Tantimongcolwat, H.J. Galla, Nanoscale orientation and lateral organization of chimeric metal-binding green fluorescent protein on lipid membrane determined by epifluorescence and atomic force microscopy, Biochem. Biophys. Res. Commun. 326 (2005) 298–306.
[10] A. Thess, S. Hutschenreiter, M. Hofmann, R. Tampe, W. Baumeister, R. Guckenberger, Specific orientation and two-dimensional crystallization of the proteasome at metal-chelating lipid interfaces, J. Biol. Chem. 277 (2002) 36321–36328.
[11] N. Bischler, F. Balavoine, P. Milkereit, H. Tschochner, C. Mioskowski, P. Schultz, Specific interaction and two-dimensional crystallization of histidine tagged yeast RNA polymerase I on nickel-chelating lipids, Biophys. J. 74 (1998) 1522–1532.
[12] M. Chalfie, Y. Tu, G. Euskirchen, W.W. Ward, D.C. Prasher, Green fluorescent protein as a marker for gene expression, Science 263 (1994) 802–805.
[13] S.R. Kain, M. Adams, A. Kondepudi, T.T. Yang, W.W. Ward, P. Kitts, Green fluorescent protein as a reporter of gene expression and protein localization, Biotechniques 19 (1995) 650–655.
[14] S. Welsh, S.A. Kay, Reporter gene expression for monitoring gene transfer, Curr. Opin. Biotechnol. 8 (1997) 617–622.
[15] R.Y. Hampton, A. Koning, R. Wright, J. Rine, In vivo examination of membrane protein localization and degradation with green fluorescent protein, Proc. Natl. Acad. Sci. USA 93 (1996) 828–833.
[16] B. Cormack, Green fluorescent protein as a reporter of transcription and protein localization in fungi, Curr. Opin. Microbiol. 1 (1998) 406–410.
[17] N. Garamszegi, Z.P. Garamszegi, M.S. Rogers, S.J. DeMarco, E.E. Strehler, Application of a chimeric green fluorescent protein to study protein–protein interactions, Biotechniques 23 (1997) 864–866, 868–870, 872.
[18] J.W. Choi, Y.S. Nam, H.G. Choi, W.H. Lee, D. Kim, M. Fujihira, Photoinduced electron transfer in GFP/viologen/TCNQ structured hetero-LB film, Synthetic Met. 126 (2002) 159–163.
[19] S.Y. Oh, J.K. Park, C.B. Ko, J.W. Choi, Patterning of photosensitive polyimide LB film and its application in the fabrication of biomolecular microphotodiode array, Biosens. Bioelectron. 19 (2003) 103–108.
[20] J.N. Volle, G. Chambon, A. Sayah, C. Reymond, N. Fasel, M.A. Gijs, Enhanced sensitivity detection of protein immobilization by fluorescent interference on oxidized silicon, Biosens. Bioelectron. 19 (2003) 457–464.
[21] V. Prachayasittikul, C. Isarankura Na Ayudhya, S. Boonpangrak, H.J. Galla, Lipid-membrane affinity of chimeric metal-binding green fluorescent protein, J. Membr. Biol. 200 (2004) 47–56.
[22] S. Stanley, C.J. Percival, M. Auer, A. Braithwaite, M.I. Newton, G. McHale, W. Hayes, Detection of polycyclic aromatic hydrocarbons using quartz crystal microbalances, Anal. Chem. 75 (2003) 1573–1577.
[23] A. Janshoff, H.J. Galla, C. Steinem, Piezoelectric mass-sensing devices as biosensors—an alternative to optical biosensors?, Angew. Chem. Int. Ed. Engl. 39 (2000) 4004–4032.
[24] A. Janshoff, C. Steinem, M. Sieber, A. el Baya, M.A. Schmidt, H.J. Galla, Quartz crystal microbalance investigation of the interaction of bacterial toxins with ganglioside containing solid supported membranes, Eur. Biophys. J. 26 (1997) 261–270.
[25] K.A. Marx, Quartz crystal microbalance: a useful tool for studying thin polymer films and complex biomolecular systems at the solution–surface interface, Biomacromolecules 4 (2003) 1099–1120.
[26] M. Bergkvist, J. Carlsson, S. Oscarsson, Surface-dependent conformations of human plasma fibronectin adsorbed to silica, mica, and hydrophobic surfaces, studied with use of atomic force microscopy, J. Biomed. Mater. Res. A 64 (2003) 349–356.
[27] F. MacRitchie, Spread monolayers of proteins, Adv. Colloid Interface Sci. 25 (1986) 341–385.
[28] V. Prachayasittikul, C. Isarankura Na Ayudhya, M. Mejare, L. Bulow, Construction of a chimeric histidine6-green fluorescent protein: role of metal on fluorescent characteristic, Thammasat Int. J. Sci. Tech. 5 (2000) 61–68.
[29] V. Prachayasittikul, C. IsarankuraNa Ayudhya, L. Bulow, Lighting *E. coli* cells as biological sensors for Cd^{2+}, Biotechnol. Lett. 23 (2001) 1285–1291.
[30] M. Ross, S. Krol, A. Janshoff, H.J. Galla, Kinetics of phospholipid insertion into monolayers containing the lung surfactant proteins SP-B or SP-C, Eur. Biophys. J. 31 (2002) 52–61.
[31] A. Eing, A. Janshoff, H.J. Galla, C. Block, C. Steinem, Quantification of the Raf-C1 interaction with solid-supported bilayers, Chembiochem 3 (2002) 190–197.
[32] C. Steinem, A. Janshoff, W.P. Ulrich, M. Sieber, H.J. Galla, Impedance analysis of supported lipid bilayer membranes: a scrutiny of different preparation techniques, Biochim. Biophys. Acta 1279 (1996) 169–180.

[33] E. Neumann, K. Tonsing, P. Siemens, Perspectives for microelectrode arrays for biosensing and membrane electroporation, Bioelectrochemistry 51 (2000) 125–132.
[34] S.F. Sui, Y.T. Sun, L.Z. Mi, Calcium-dependent binding of rabbit C-reactive protein to supported lipid monolayers containing exposed phosphorylcholine group, Biophys. J. 76 (1999) 333–341.
[35] J.P. Rieu, F. Ronzon, B. Roux, Adsorption and aggregation of glycosylphosphatidyl inositol (GPI) anchored alkaline phosphatase on methylated glass surfaces studied by tapping mode atomic force microscopy, Thin Solid Films 406 (2002) 241–249.
[36] M. Teresa, S.R. Gomes, K.S. Tavares, J.A. Oliveira, The quantification of potassium using a quartz crystal microbalance, Analyst 125 (2000) 1983–1986.
[37] M.T. Gomes, K.S. Tavares, J.A. Oliveira, Development of a sensor for calcium based on quartz crystal microbalance, Fresenius J. Anal. Chem. 369 (2001) 616–619.
[38] N. Matsuura, D.J. Elliot, N.D. Ferlong, F. Grieser, In-situ measurement of lead (II) ion binding to an arachidic acid langmuir monolayer using a quartz crystal microbalance, Colloid. Surface. 126 (1997) 189–195.